Acceleration Control of a Multi-Rotor UAV with Disturbance Observer against Wind

A Dissertation

by

SEUNG JAE LEE

Presented to the Faculty of the Graduate School of
Seoul National University
in Partial Fulfillment
of the Requirements
for the Degree of

MASTER OF SCIENCE

School of Mechanical & Aerospace Engineering

Seoul National University

Supervisor : Professor H. Jin Kim

December 2015

to my

FATHER, whom my lighthouse

MOTHER, the port that I always anchors

SISTER, the lifelong companion and the best advisor

with love

Do not go gentle into that good night,
Old age should burn and rave at close of day;
Rage, rage against the dying of the light.

-Dylan Thomas-

Abstract

Acceleration Control of a Multi-Rotor UAV with Disturbance Observer against Wind

Seung Jae Lee
Department of Mechanical & Aerospace Engineering
The Graduate School
Seoul National University

In In this dissertation, the control method of the hexarotor unmanned aerial vehicle that flies in an outdoor environment is presented. Flight in an outdoor environment is different than in an indoor environment due to the atmospheric disturbances such as wind or gust that generate unwanted planar acceleration to the airframe. In order to compensate the effect generated by the atmospheric disturbance, two modifications compared to the conventional position control is introduced. One is the planar acceleration control, and the other is the disturbance observer algorithm applied into the planar acceleration controller that cancels the atmospheric disturbance out. First, the transformation matrix between the attitude and the planar acceleration is derived. With the transformation matrix, it is possible to calculate the desired attitude for the generation of the desired planar acceleration. Since the hexarotor unmanned aerial vehicle follows the desired attitude well with help of the fine operating attitude controller, the control of the airframe's planar acceleration also makes a fine performance. After the planar acceleration control, the 'disturbance observer' method is applied. Finding the transfer function between the desired planar acceleration command and the outcome planar acceleration, the calculation of the estimated desired planar acceleration command could be done by the multiplication of the current planar acceleration and the inverse of the transfer function. Comparing the calculated estimated desired planar acceleration command and the actual planar acceleration command, estimated disturbance could be calculated. Substracting the estimated disturbance value in next control loop's desired planar acceleration command, it is possible to generate adequate command that flies with intended planar acceleration canceling out the outer disturbances. For stability analysis, the small gain

theorem is used. With the small gain theorem, the bandwidth of the low pass filter for the stability of the entire disturbance observer system could be set. Both simulation and actual experiment has been done for the validation of the control method.

Keyword : Hexarotor, Multi-rotor unmanned aerial vehicle, Robust control, Disturbance observer, Acceleration control, Small gain theorem

Student Number : 2014-20678

Table of Contents

Page

Abstract iii

Table of Contents v

List of Figures vii

List of Tables viii

Chapter

1 Introduction 1

1.1 Literature Review 2

1.2 Thesis Contribution 3

2 Hexarotor Modeling 4

2.1 Hexarotor Configuration 4

2.2 Kinematics and Dynamics 6

2.3 Modelling of the Hexarotor 8

3 Acceleration Control of UAV 10

3.1 Control Strategy 10

3.2 Acceleration Control of UAV 11

4 Disturbance Observer 13

4.1 Disturbance Observer based Acceleration Control 13

5 Stability Analysis 16

5.1 Simplification of the Block Diagram 16

5.2 Stability Analysis: Theory 17

5.3 Stability Analysis: Application to the Real Plant 19

6 Simulation Result 22

7 Experimental Result 26

7.1 Hardware Introduction and Experiment Settings 26

7.2 Experimental Result 27

8 Conclusion 30

References 31

List of Figures

1.1 Example of a small-sized(left) and a large-sized(right) quadrotor UAV 2

2.1 The relationship between PWM signal and motor thrust 5

2.2 Visual motion description of the hexarotor UAV 6

2.3 Attitude control structure of the hexarotor UAV 9

3.1 Acceleration control structure of the hexarotor UAV 12

4.1 Position control structure of the haxarotor with proposed DOB structure 14

5.1 $||a||$ block replacing G (left), simplified (middle), equivalent single feedback loop (right) 17

5.2 Block diagram with P and C(left), filled form of the P and C block (middle), equivalent form (right) 18

5.3 Comparison between desired acceleration command and current acceleration(left), same result but delaying desired command 0.4 seconds(right) 20

5.4 Bode diagram of the Δ^{-1} and Q with various τ values 21

6.1 Still cut image of the hexarotor UAV's simulation flight(left), flight control structure composed in Matlab simulink(right) 22

6.2 Comparison between hexarotor UAV's desired and current states: no DOB(upper left), with DOB(upper right), attitude trajectory: no DOB(lower left), with DOB(lower right) 24

6.3 Comparison of the real disturbance and the estimated disturbances 25

7.1 The hexarotor UAV used in experiment(left), still cut image of experiment(right) . 27

7.2 Position log of desired and current position w and w/o acceleration DOB 28

7.3 Estimated disturbance(left), raw and DOB applied acceleration command(right) . 29

List of Tables

7.1 Main specifications of the hexarotor UAV used in experiment 27

1 Introduction

MULTI-ROTOR drone in nowadays is being used with various purposes. Some small scale drones for example, are made for indoor toy flight that agile movement due to its small rotational inertia gives operator exciting hobby experiences. Middle or large scale drones are widely used as platform for outdoor data acquisition such as image achievement with attached camera or 3-D environment scanning with LIDAR sensor. Because it needs to carry relatively heavy sensing and navigating equipment, high performance propulsion system and high capacity batteries should be equipped. But even with the advantages of the high performance motor and the large propeller, outdoor flight is not easy to have satisfactory performance because of the atmospheric interference such as gust, or wind. Especially when operator wants drone to move or hover with precise path or position, atmospheric interference directly generates unwanted inertial acceleration that makes drone to off course. To deal with the atmospheric interference, many researchers found ways to solve this problem in rigid attitude control. Methods with tuning the integral gain for improved disturbance rejection in PID control or applying model predictive control in attitude control are examples. These methods are highly efficient when atmospheric disturbance is affecting control torque generation that makes hard to control drone's attitude. But when atmospheric disturbance is affecting into drone's centre of mass that 'pushes' it from one way to another, rigid attitude control cannot be a solution. To deal with this problem, first the position controller should have

Figure 1.1: Example of a small-sized(left) and a large-sized(right) quadrotor UAV

capability to control the planar acceleration of its own. After that, the controller should observe magnitude of the acceleration due to the atmospheric disturbance and compensate it. In this dissertation, the development of an inertial acceleration controller of the multi-rotor drone with disturbance observer (DOB) algorithm, which provides robustness of the controller has been done. First, configuration, kinematics and dynamics of the hexarotor UAV will be introduced. After that, the introduction of the proposed DOB structure will be shown. In the end, both simulation and experimental result will be introduced with some graphical analysis.

1.1 Literature Review

The effort of the control engineers around the world to make better performance of multi-rotor drone against disturbances can be found by massive amount of papers. In [1], the attitude control with with optimized PID parameters is introduced. Not doing a rough tuning of the parameter, they set desired performance of the controller and calculated gains. The full attitude control of a quadrotor on SO(3) field is introduced in [2]. The contribution of this paper is that they earned the controllability in SO(3) field, making more direct control. In [3], the platform is flapping-wing robot but it made a model of the wind disturbance and rejected it with control method in same dynamics. One used MPC(Model Predictive Control) method in [4],[6] with disturbance database,

feedback linearisation in [5], sliding mode approach in [7]. The result of those researches show better performance than normal PID control but still, the model-only technique has a limit.
In disturbance observer approach, almost all methods are focusing the rigid attitude control. Because the multi-rotor drone generates linear acceleration with tilting action, the powerful attitude control is important. Lee[9] applied disturbance observer for robust attitude tracking controller. With singular perturbation, the stability has been proved. The new Q-filter design that is very important for system stability is introduced in [12]. The most close concept of the application of DOB of this dissertation is [11]. It uses DOB to make rigid linear velocity control. The stability analysis in this paper is done by ISS.
Throughout papers that has been reviewed, the disturbance observer algorithm applied in acceleration control didn't exist. The main reason is because the dissertation deals about linear acceleration control that hasn't been dealt before. Since the upper controller earns the capability to control the linear acceleration, disturbance observer could engage into the linear acceleration. The basic kinematics and dynamics of the multi-rotor UAV is learned from [16], [17].

1.2 Thesis Contribution

In this dissertation, there are two main contributions.

Contribution 1: The multi-rotor UAV's linear acceleration control toward inertial x and y axis is introduced.

Contribution 2: The disturbance observer applied in the UAV's linear acceleration control, which rejects the unwanted linear acceleration is introduced.

To guarantee these contributions, the stability analysis of the overall system has been done. Both simulation and experiment also has been done for verification of this concept.

2

Hexarotor Modeling

2.1 Hexarotor Configuration

THE hexarotor unmanned aerial vehicle is a platform that contains six fixed pitch propellers generating desired acceleration to each inertial coordinate with an appropriate attitude control. Each motor follows '**propulsion to angular velocity relationship**' or $F = k\omega^2$ where $F \in \mathbb{R}$ is the propelled force and k the thrust constant of the propeller, $\omega \in \mathbb{R}$ the angular velocity of the motor[17]. Since the thrust of the rotor is related to the square of the rotation speed, we should monitor the rotation speed of each motor. But it is inefficient way for hexarotor UAV that it has very limited payload to carry additional encoder sensors. In this dissertation, without using the method of monitoring the rotational speed, we used so called '**pre-mapping method**'. Since motor is controlled by an electronic signal, we mapped the relationship between electronic signal and actual thrust generated by the motor. The Figure 2.1 shows the relationship between the PWM(Pulse Width Modulation) signal that goes into the motor controller and output thrust measured by the force sensor. The platform that is going to be shown in later section for experiment uses motor controller with PWM signal as input. So, when we measure the thrust in each PWM signal and build a simplified approximated thrust equation, we don't need to measure the rotational speed of the motor but knows the thrust. The motor that is used in this experiment is DJI's E600 motor driver set with 12 inch propeller attached. The proposed linear model from the

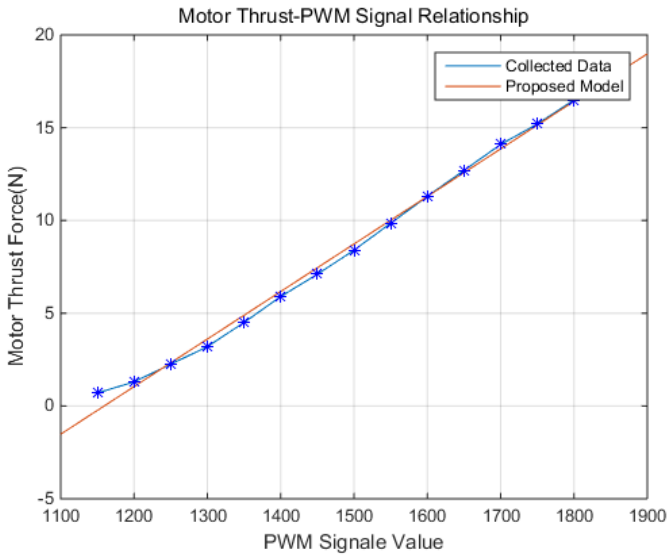

Figure 2.1: The relationship between PWM signal and motor thrust

experimental result is

$$F_{motor} = 0.025628 * [PWM] - 29.7089 \qquad (N) \tag{2.1}$$

Back to the hardware configuration, three pairs of rotors in the hexarotor turn in opposite direction in order to cancel the torque generated due to rotor rotation. Figure 2.2 describes concept motions of a hexarotor. When controlling the roll angle, force difference between (F_1, F_5, F_6) and (F_2, F_3, F_4) in Figure 2.2 generates roll torque. But when controlling the pitch angle, force difference between (F_1, F_2) and (F_4, F_5) generates pitch torque. The relationship between forces and torques are therefore given as the following equation.

$$U = \begin{bmatrix} T \\ \tau_{roll} \\ \tau_{pitch} \\ \tau_{yaw} \end{bmatrix} = \begin{bmatrix} 1 & 1 & 1 & 1 & 1 & 1 \\ \frac{\sqrt{3}}{2}l & \frac{\sqrt{3}}{2}l & 0 & -\frac{\sqrt{3}}{2}l & -\frac{\sqrt{3}}{2}l & 0 \\ \frac{b}{k} & -\frac{b}{k} & \frac{b}{k} & -\frac{b}{k} & \frac{b}{k} & -\frac{b}{k} \\ -\frac{1}{2}l & \frac{1}{2}l & l & \frac{1}{2}l & -\frac{1}{2}l & -l \end{bmatrix} \begin{bmatrix} F_1 \\ F_2 \\ F_3 \\ F_4 \\ F_5 \\ F_6 \end{bmatrix} = Z(b, k, l)\Pi \tag{2.2}$$

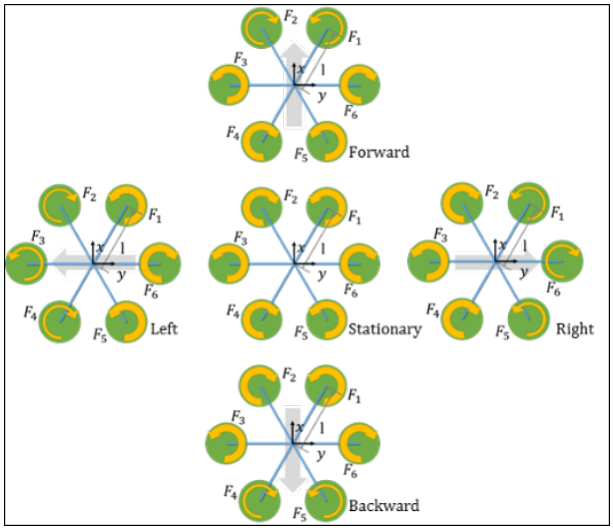

Figure 2.2: Visual motion description of the hexarotor UAV

where $U \in \mathbb{R}^4$ is the thrust set matrix, τ is the torque generated due to the propellers, T stands for the total thrust, k is the propeller's thrust constant and b is the propeller's drag constant and Π is the thrust force matrix.[16]

The $Z(b, k, l)$ matrix is used in hexarotor control since the attitude controller and the thrust controller generate desired thrust and desired roll, pitch, yaw moment, which is U. The force that each motor should propel than should be

$$\Pi_{des} = Z(b, k, l)^{-1} U_{des} \tag{2.3}$$

Once we know the relationship between thrust of the motor and PWM signal shown in equation(2.1), we can easily calculate how much PWM signal does each motor need to generate desired thrust.

The methodology of the generation of U_{des} will be dealt in later section.

2.2 Kinematics and Dynamics

The position and attitude kinematics of the hexarotor is given by

$$\dot{X} = R(\theta)V \tag{2.4}$$

$$\dot{\theta} = W(\theta)\Omega \tag{2.5}$$

where $X = [x, y, z]^T \in \mathbb{R}^3$ is the inertial coordinate position of the drone and $V = [u, v, w]^T \in \mathbb{R}^3$ is the linear velocity in body-fixed frame.[5] $\Theta = [\phi, \theta, \psi]^T \in \mathbb{R}^3$ denotes the attitude in Euler angle and $\Omega = [p, q, r]^T \in \mathbb{R}^3$ is the angular velocity of the drone in body-fixed frame. Matrix $R(\Theta) \in \mathbb{R}^{3\times3}$ and $W(\Theta) \in \mathbb{R}^{3\times3}$ are as follows.

$$R(\Theta) = \begin{bmatrix} \cos\phi\cos\psi & \sin\phi\sin\theta\cos\psi - \cos\phi\sin\psi & \cos\phi\sin\theta\cos\psi + \sin\phi\sin\psi \\ \cos\phi\sin\psi & \sin\phi\sin\theta\sin\psi + \cos\phi\cos\psi & \cos\phi\sin\theta\sin\psi - \sin\phi\cos\psi \\ -\sin\theta & \sin\phi\cos\theta & \cos\phi\cos\theta \end{bmatrix} \tag{2.6}$$

$$W(\Theta) = \begin{bmatrix} 1 & \sin\phi\tan\theta & \cos\phi\tan\theta \\ 0 & \cos\phi & -\sin\phi \\ 0 & \frac{\sin\phi}{\cos\theta} & \frac{\cos\phi}{\cos\theta} \end{bmatrix} \tag{2.7}$$

The dynamics of the hexarotor UAV is as follows. First, attitue dynamics of the hexarotor is given by

$$\mathrm{T} = J\dot{\Omega} + \Omega \times (J\Omega) \tag{2.8}$$

where $\mathrm{T} = [\tau_{roll}, \tau_{pitch}, \tau_{yaw}]^T \in \mathbb{R}^3$ is the torque applied into airframe, $J \in \mathbb{R}^{3\times3}$ the moment of inertia matrix. Second, the position dynamics of the hexarotor is given by

$$\ddot{\mathrm{X}} = g \begin{bmatrix} 0 \\ 0 \\ 1 \end{bmatrix} - R(\Theta)\frac{(\sum_{i=1}^{n} F_i)}{m} \begin{bmatrix} 0 \\ 0 \\ 1 \end{bmatrix} \tag{2.9}$$

where g is the gravitational acceleration and m is the total mass of the hexarotor UAV. So the overall dynamics model can be written as

$$\ddot{x} = -\frac{u_1}{m}(\cos\phi\sin\theta\cos\psi + \sin\phi\sin\psi) \tag{2.10}$$

$$\ddot{y} = -\frac{u_1}{m}(\cos\phi\sin\theta\sin\psi - \sin\phi\cos\psi) \tag{2.11}$$

$$\ddot{z} = g - \frac{u_1}{m}(\cos\phi\cos\theta) \tag{2.12}$$

$$\ddot{\phi} = \dot{\theta}\dot{\psi}(\frac{\mathrm{I}_y - \mathrm{I}_z}{\mathrm{I}_x}) - \frac{\mathrm{I}_R}{\mathrm{I}_x}\dot{\theta}(\omega_1 - \omega_2 + \omega_3 - \omega_4 + \omega_5 - \omega_6) + \frac{l}{l_x}u_2 \tag{2.13}$$

$$\ddot{\theta} = \dot{\phi}\dot{\psi}(\frac{\mathrm{I}_z - \mathrm{I}_x}{\mathrm{I}_y}) + \frac{\mathrm{I}_R}{\mathrm{I}_y}\dot{\phi}(\omega_1 - \omega_2 + \omega_3 - \omega_4 + \omega_5 - \omega_6) + \frac{l}{l_y}u_3 \tag{2.14}$$

$$\ddot{\phi} = \dot{\phi}\dot{\theta}(\frac{\mathrm{I}_x - \mathrm{I}_y}{\mathrm{I}_z}) + \frac{l}{l_z}u_4 \tag{2.15}$$

2.3 Modelling of the Hexarotor

When the hexarotor UAV needs to maintain its altitude, independently operating height controller calculates u_1 value to keep its altitude. From equation (2.12), considering $\ddot{z}$ as near 0 in hovering state, total thrust should be $u_1 = \frac{mg}{\cos\phi\cos\theta}$. This means that high value of the roll and pitch angle makes u_1 so big that the hexarotor drone cannot generate enough power to keep its altitude. Because of this reason, we must control drone's attitude with small boundary. This limit gives us a legitimacy of small angle assumption, which means that we can treat $\cos\phi \approx 1, \cos\theta \approx 1, \sin\phi \approx \phi$ and $\sin\theta \approx \theta$.

Reminding from the equation (2.8), attitude dynamics of the hexarotor is composed with the inertial moment term and the gyroscopic term. But the gyroscopic effect is so small in conventional drone size that we can simply neglect it. Applying the small angle assumption, matrix W in equation (2.7) can be treated as $W \approx I \in \mathbb{R}^{3\times3}$, making the transfer function of the drone's dynamics as

$$\mathrm{T} = J\dot{\Omega} = J(W^{-1})^2(W\ddot{\Theta} - \dot{W}\dot{\Theta}) = J\ddot{\Theta} \tag{2.16}$$

The rotational inertial moment J is near diagonal matrix, which non-diagonal component of the matrix is so small compared to diagonal components. So, as shown in the Figure 2.3's attitude

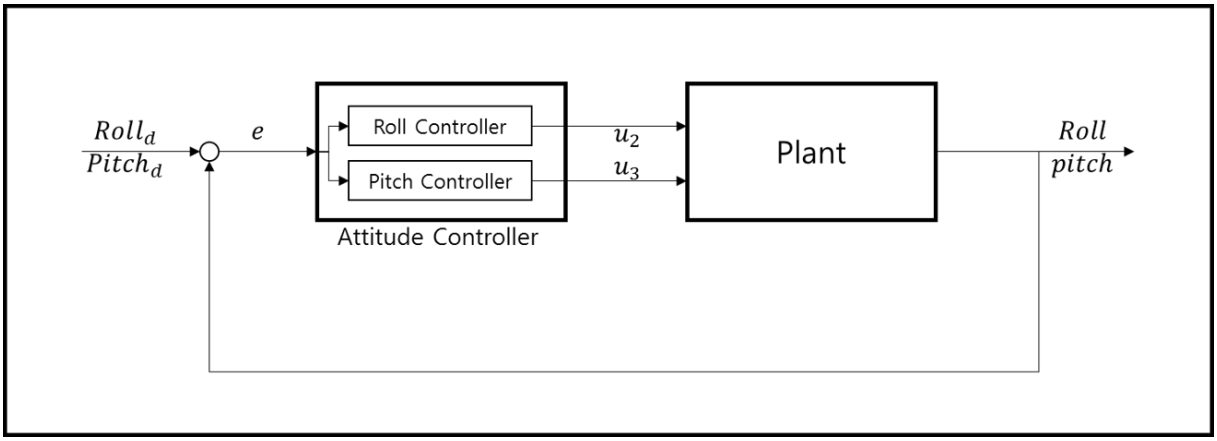

Figure 2.3: Attitude control structure of the hexarotor UAV

controller block, we can think the roll and pitch attitude is independent to each other. Using PID controller for attitude control, the transfer function of the 'desired-current attitude' is

$$\frac{\Theta(s)}{e(s)} = \frac{T_{pitch}(s)}{D(s) - \Theta(s)} \frac{\theta(s)}{T_{pitch}(s)} = \frac{Ps + I + Ds^2}{s} \frac{1}{J_{pitch}s^2} = \frac{Ps + I + Ds^2}{J_{pitch}s^3} \tag{2.17}$$

$$\Lambda_n(s) = \frac{\Theta(s)}{D(s)} = \frac{Ds^2 + Ps + I}{Js^3 + Ds^2 + Ps + I} \tag{2.18}$$

where $\Lambda_n(s)$ is the nominal transfer function between desired and current attitude. As we can see, the system is 3rd order with relative degree 1.

3

Acceleration Control of UAV

The acceleration of the hexarotor UAV is generated only from the propulsion of rotors attached vertically into the airframe. Thus, in order to generate desired acceleration to certain direction, airframe should be tilted to certain direction. In other words, one needs to find the relationship between the acceleration of the airframe and its attitude to control the acceleration of the UAV. In this chapter, we will find the relationship between the inertial linear acceleration and the attitude so that we can calculate desired attitude to generate desired linear acceleration.

3.1 Control Strategy

Throughout this dissertation, we will control the hexarotor UAV with three independent controllers. One is the '**Position controller set**' that contains inertial position controller and attitude controller. Another is the '**Height controller**', controlling the total thrust to maintain desired altitude. The other is the '**Heading angle controller**', which controls drone's facing direction. The reason of these separation is because control states of each controller commands are highly decoupled to each other.

3.2 Acceleration Control of UAV

Considering the result of the small angle assumption applied into the hexarotor drone's dynamics, we can rewrite the inertial acceleration dealt in equation (2.10),(2.11),(2.12) as

$$\ddot{x} = -\frac{u_1}{m}(\theta \cos\psi + \phi \sin\psi) \tag{3.1}$$

$$\ddot{y} = -\frac{u_1}{m}(\theta \sin\psi - \phi \cos\psi) \tag{3.2}$$

$$\ddot{z} = g - \frac{u_1}{m} \tag{3.3}$$

As mentioned previously, the height control of the hexarotor drone is operated independently. So u_1 the total thrust, which is $u_1 = ||R(\Theta)[0 \quad 0 \quad \Sigma F]^T|| = m||a||$, is controlled by the height controller. Therefore, in the position controller's point of view, $||a||$ can be treated as given value. Rewriting it, we can simpliy the equation (3.1), (3.2) as

$$\frac{\mathrm{d}^2}{\mathrm{dt}^2}\begin{bmatrix} x \\ y \end{bmatrix} = G(||a||, \psi)\begin{bmatrix} \phi \\ \theta \end{bmatrix} \tag{3.4}$$

where

$$G(||a||, \psi) = -||a||\begin{bmatrix} \sin\psi & \cos\psi \\ -\cos\psi & \sin\psi \end{bmatrix} \tag{3.5}$$

From this equation, we can derive the '**inertial acceleration - attitude angle**' relationship with given norm of the current acceleration and yaw. This means when the controller wants the drone to move with desired x and y directional acceleration, the signal could be converted into the desired roll and pitch angle. With the combination of the attitude controller that we have dealt in previous section, x and y acceleration in inertial coordinate is controllable with below equation's relationship.

$$\begin{bmatrix} \phi_{des} \\ \theta_{des} \end{bmatrix} = G(||a||, \psi)^{-1}\begin{bmatrix} \ddot{x}_{des} \\ \ddot{y}_{des} \end{bmatrix} \tag{3.6}$$

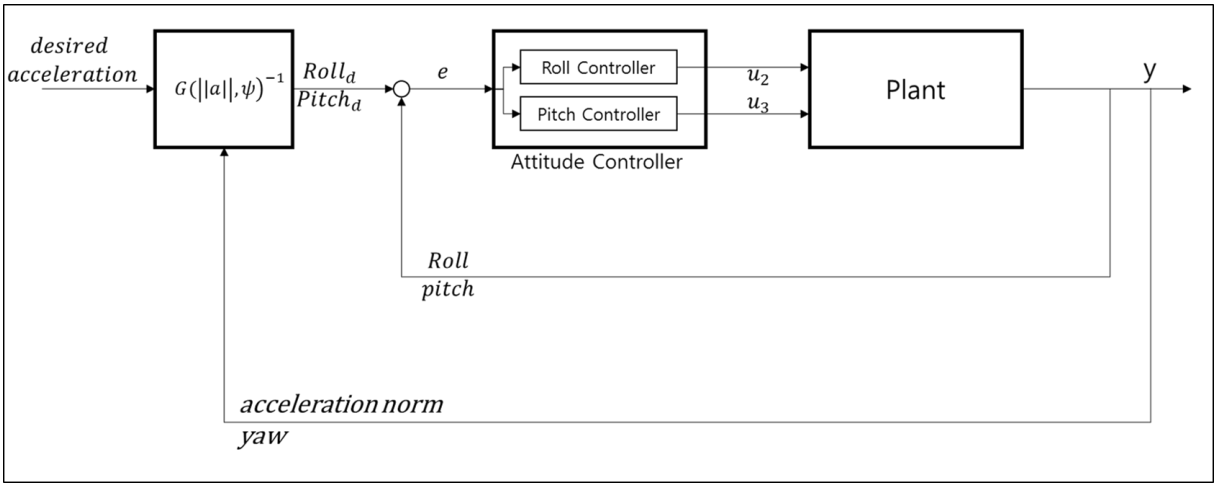

Figure 3.1: Acceleration control structure of the hexarotor UAV

So, when controller wants drone to move with desired direction, the G matrix that is updated with current norm of the acceleration and yaw angle transforms it into desired roll and pitch angle. After than, the attitude controller controls the thrust of each motor to move the hexarotor drone into desired attitude. The block diagram of the inertial acceleration controller is shown in Figure 3.1.

4

Disturbance Observer

In this chapter, the disturbance observer algorithm applied into the acceleration control will be introduced. The aim of this chapter is to build the control structure that reduces the effect of disturbances generated by the atmospheric activity, which gives direct effect to the airframe's inertial acceleration generation. To achieve this goal, we need to treat the '**hexarotor UAV with an attitude controller**' as single system block that generates desired linear acceleration. It means that we need to treat the hexarotor UAV's dynamics and the feedback attitude controller as single transfer function. This concept is very useful to linear acceleration disturbance observer, because disturbance observer only uses desired acceleration and current acceleration for wind-caused disturbance estimation. So, we define the '**hexarotor UAV with an attitude controller**' as '**Inner Loop** $\Lambda_p(s)$'. In Figure 4.1, the blue box shows an inner loop $\Lambda_p(s)$ that acceleration controller should control.

4.1 Disturbance Observer based Acceleration Control

The disturbance affecting the hexarotor's inertial coordinate acceleration control goes into the body frame directly. But the effect of the disturbance can be converted into the equivalent disturbance command d in Figure 4.1 that contaminates desired acceleration right after u. In this section, the DOB based inertial acceleration control method will be introduced. As typical DOB structures

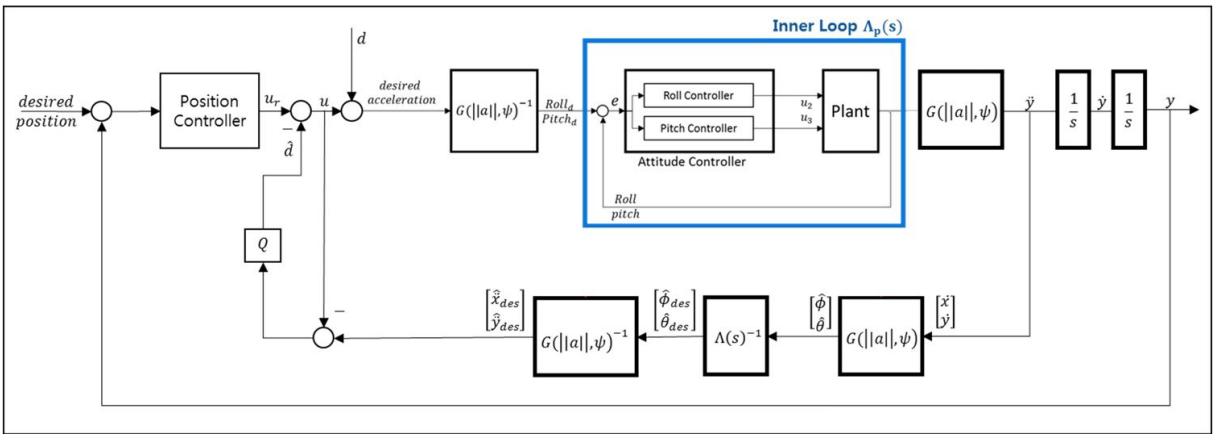

Figure 4.1: Position control structure of the haxarotor with proposed DOB structure

have, the acceleration DOB consists of two parts; one is the estimation of the unwanted disturbance, and the other is the rejection of the unwanted disturbance by adding a compensation signal to control input. First, for disturbance estimation in DOB structure, INS(Inertial Navigation System) sensor attached in the airframe measures the inertial acceleration $\ddot{X} = [\ddot{x}\ \ddot{y}]^T \in \mathbb{R}^2$. Then, we calculate the estimated current roll and pitch angle as $\hat{\Theta} = G(||a||, \psi)\ddot{X}$. After that, the estimated desired roll and pitch angle $\hat{\Theta}_{des}$ can be calculated as $\hat{\Theta}_{des} = \Lambda_n(s)^{-1}\hat{\Theta}$ with $\hat{\Theta} = [\hat{\phi}_{des}\ \hat{\theta}_{des}]^T \in \mathbb{R}^2$ since $\Lambda_n^{-1}(s)$ is the nominal inverse of the inner loop transfer function that is the relationship between current attitude and the resulting desired attitude. Multiplying $G(||a||, \phi)^{-1}$ the inverse of the attitude to acceleration transfer matrix and $\hat{\Theta}_{des} = [\hat{\phi}_{des}\ \hat{\theta}_{des}]^T \in \mathbb{R}^2$, the estimated desired inertial x and y axial acceleration $\hat{\ddot{X}}_{des} = [\hat{\ddot{x}}_{des},\ \hat{\ddot{y}}_{des}]^T$ can be calculated as follows.

$$\hat{\ddot{X}}_{des} = \begin{bmatrix}\hat{\ddot{x}}_{des}\\ \hat{\ddot{y}}_{des}\end{bmatrix} = G(||a||, \psi)^{-1}\Lambda(s)^{-1}G(||a||, \psi)\begin{bmatrix}\ddot{x}\\ \ddot{y}\end{bmatrix} = G(||a||, \psi)^{-1}\Lambda(s)^{-1}\begin{bmatrix}\phi\\ \theta\end{bmatrix} \tag{4.1}$$

The $G(||a||, \psi)[\ddot{x}, \ddot{y}]^T$ in equation (4.1) can be replaced to $[\phi, \theta]^T$ because it is the estimated current attitude. The current attitude could be measured by INS sensor directly.

Since the $\hat{\ddot{X}}_{des}$ is the estimated desired axial acceleration command that caused current axial acceleration result, the value contains not only $\hat{u}_r$ the estimated desired acceleration coming from the '**Position Controller**' in Figure 4.1, but also $\hat{d}$ the estimated equivalent disturbance

command. In equation,

$$\hat{\ddot{X}}_{des} = \hat{u}_r + \hat{d} \tag{4.2}$$

. So subtracting u the command coming from the '**Position Controller**' from $\hat{\ddot{X}}_{des}$ is

$$\hat{\ddot{X}}_{des} - u = (\hat{u}_r + \hat{d}) - u \approx \hat{d} \tag{4.3}$$

where $\hat{d}$ is the lumped estimated disturbance. If we subtract $\hat{d}$ from u_r in next control step, final input command u becomes $u_r - \hat{d}$. The equivalent disturbance input d is added to u after than. The final command therefore becomes $(u_r - \hat{d}) + d \approx u_r$ in ideal situation. Refer Figure 4.1.
The nominal transfer function $\Lambda_n(s)$ is minimum phase, linear time-invariant system whose relative degree is $r \geq 1$. So, the $\Lambda_n^{-1}(s)$ used in the calculation of $\hat{d}$, is improper function that brings unstable result due to its self-contained pure differentiator trait. To suppress it for stable estimation result, we put additional filter called Q-filter with relative degree higher than r that makes overall transfer function proper. The Q-filter is generally designed as

$$Q(s) = \frac{b_k(\tau s)^k + b_{k-1}(\tau s)^{k-1} + \cdots + b_0}{(\tau s)^l + a_{l-1}(\tau s)^{l-1} + \cdots + a_1(\tau s) + a_0} \tag{4.4}$$

where $l \geq k + r$ and $b_0 = a_0$ so that value of Q is 1 when s is 0.[15] The bandwidth of the Q filter is very important because it determines the entire stability of the system. The stability analysis in next chapter is about the method for determination of the bandwidth of filter Q.

5

Stability Analysis

BEFORE starting the stability analysis of the proposed control algorithm, first we need to apply some reasonable assumptions to simplify the analysis since the system dynamics contains non-linear components that makes the analysis uneasy. For simplification, two assumptions are applied.

Assumption 1: The UAV maintains zero degree heading angle during entire flight controlled by independently operating heading angle controller.
Assumption 2: The roll and pitch angle of the hexarotor UAV during entire flight is relatively small that the small angle assumption keeps its validity.

In this chapter, we are going to find the boundary of the tunable parameters, especially the bandwidth of the Q filter introduced in chapter 4, to guarantee the stability of the system with help of those two assumptions.

5.1 Simplification of the Block Diagram

The main reason of the '**Assumption 1**' is to neutralize the non-linear triangular components in G matrix of equation (3.5). The G matrix is composed with two components: norm of the acceleration and heading angle ψ. When ψ maintains zero heading angle during entire flight, the

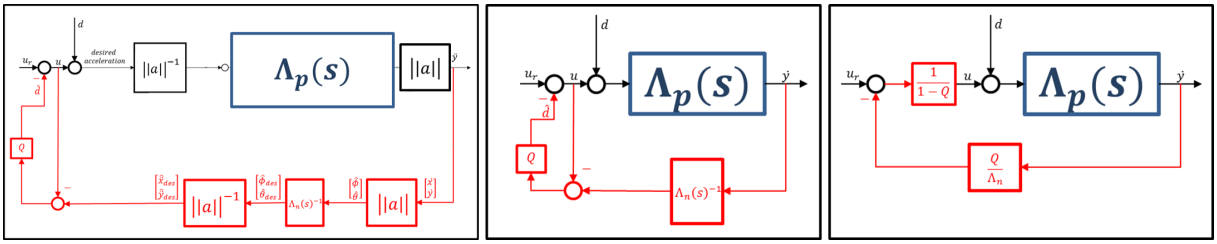

Figure 5.1: $||a||$ block replacing G (left), simplified (middle), equivalent single feedback loop (right)

G matrix becomes as equation (5.1).

$$G(||a||, \psi) = -||a|| \begin{bmatrix} 0 & 1 \\ -1 & 0 \end{bmatrix} \tag{5.1}$$

This means the independence of the roll and pitch angle that each angle controls the x and y acceleration separately. This also means that multiplication of $||a||$ the norm of the acceleration to the current attitude angle becomes airframe's axial acceleration during the $\psi = 0$ condition keeps its validity. Thus, we can pick one of the attitude component(ex. roll) to carry out stability analysis of the entire system because the independence of each attitude component guarantees the other component's stability. The G matrix than can be changed into $||a||$ multiplication block in single attitude component shown in Figure 5.1(left). The $||a||$ and $||a||^{-1}$ function block located in forward and backward of the $\Lambda_p(s)$ and $\Lambda_n^{-1}(s)$ could be cancelled. Reduced structure of Figure 5.1(left) is shown in Figure 5.1(middle). The very left loop section of the Figure 5.1(middle) containing the Q filter can be removed by adding $(1-Q)^{-1}$ block and changing $\Lambda_n^{-1}(s)$ to $Q\Lambda_n^{-1}(s)$ as shown in Figure 5.1(right).

The reason of the '**Assumption 2**' is for validity of the small angle assumption that has been explained in chapter 3.2. So the explanation will be skipped in this section.

5.2 Stability Analysis: Theory

For the stability analysis of the proposed system, small gain theorem has been chosen.[15] The hexarotor UAV's dynamics model is considered as 'pure delay model' in this analysis since the actual plant response can be described as pure delay of nominal response. In equation, the pure

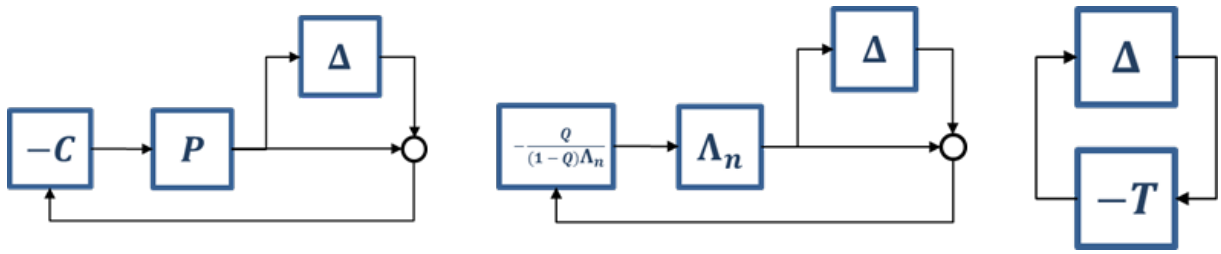

Figure 5.2: Block diagram with P and C(left), filled form of the P and C block (middle), equivalent form (right)

delay model could be written as

$$\Lambda_p(s) = \Lambda_n(s)e^{-sT_d} \tag{5.2}$$

where $\Lambda_n(s)$ is the nominal model of the hexarotor UAV dealt in equation (2.18) and $\Lambda_p(s)$ is actual plant model with pure delay. T_d stands for the time delay between nominal and real model. The T_d will be measured by real experiment shown in later section.

For the application of the small gain theorem, we will treat the real plant model $\Lambda_p(s)$ as multiplicative perturbation model. In equation, the multiplicative perturbation model could be written as equation (5.3).

$$\Lambda_p(s) = \Lambda_n(s)(1 + \Delta) \tag{5.3}$$

With equation (5.2) and equation (5.3), the Δ can be calculated as

$$\Delta = e^{-sT_d} - 1 \tag{5.4}$$

In multiplicative perturbation model, the block diagram of the structure is as shown in Figure 5.2(left). Matching the structure to DOB applied structure in Figure 5.1(right), we can derive that C and P block in Figure 5.2(left) as $-\frac{Q}{(1-Q)\Lambda_n}$ and Λ_n respectively. Refer Figure 5.2(middle). The structure in Figure 5.2(middle) can be simplified into two blocks: The Δ, and $-T$. The T is called

'**Complimentary Sensitivity Function**' and is calculated as

$$T = \frac{PC}{1+PC} = \frac{\Lambda_n \frac{Q}{(1-Q)\Lambda_n}}{1+\Lambda_n \frac{Q}{(1-Q)\Lambda_n}} = Q \tag{5.5}$$

The application of the small gain theorem derives the inequality equation shown below.

$$||\Delta \cdot T||_\infty = ||\Delta \cdot Q||_\infty < 1 \tag{5.6}$$

The equation(5.6) is called '**Small Gain Theorem**' that if infinite norm of the multiplication of two blocks are less than 1, the system should be stable.[15] The Δ and Q has four parameters (T_d, a_0, a_1, τ). But for T_d, a_0 and a_1, we can treat those three as pre-set values. Therefore, we only need to find adequate range of τ to ensure the stability of the system.[15]

5.3 Stability Analysis: Application to the Real Plant

The parameters in this inequality equation are T_d, a_0, a_1, τ. T_d is the time delay between nominal plant and real plant. So, when we measure T_p the time delay between desired and real plant response and T_n the time delay between desired and nominal plant response and subtract it, we can measure the T_d. In equation, T_d is as equation (5.7).

$$T_d = T_p - T_n \tag{5.7}$$

a_0 and a_1 value in Q-filter is selected to 1 and 2 respectively with discretion.
T_n can be measured by the comparison of command and response calculated using Λ_n transfer function. The value has been measured approximately 0.3 seconds. T_p can be measured by actual experimental result. The Figure 5.3(left) shows manual flight result of hexarotor UAV. Red line represents the desired axial acceleration and blue line represents the resulting acceleration measured by on-board IMU. The Figure 5.3(right) shows the same result but moving the red command log to 0.4 seconds right side using pade approximation. The phase of the red and blue line seems to be matched. Therefore, we can estimate the T_p value about 0.4 seconds. With equation (5.7), the T_d value is about 0.1 seconds and therefore, $\Delta = e^{-0.1s} - 1$. Based on equation (5.6),

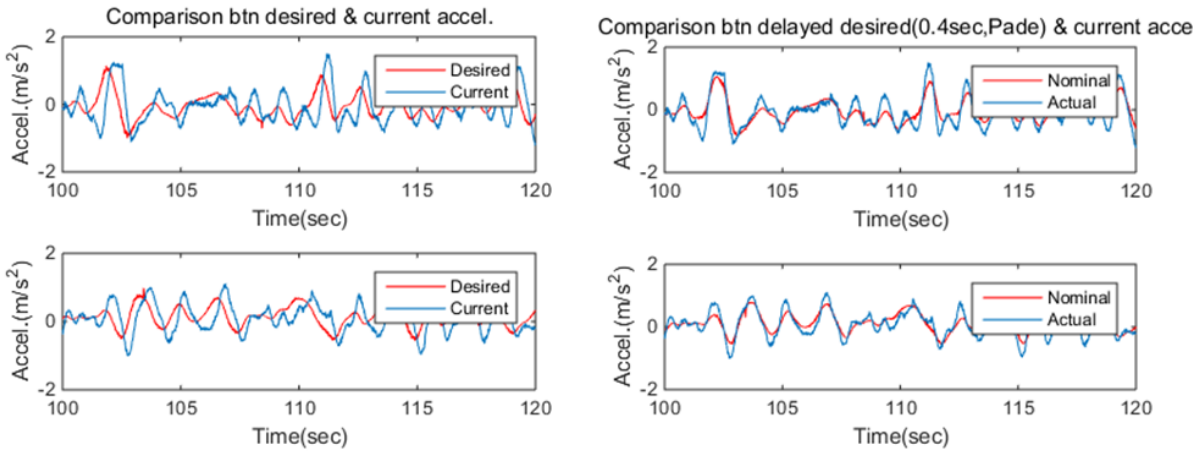

Figure 5.3: Comparison between desired acceleration command and current acceleration(left), same result but delaying desired command 0.4 seconds(right)

we should find the boundary of τ that satisfies the inequality equation.

The equation (5.7) can be rewritten as equation (5.8).

$$||Q(s)||_\infty < \frac{1}{||\Delta(s)||_\infty} \tag{5.8}$$

The Figure 5.4 shows the Bode diagram of $\Delta^{-1}(s)$ and $Q(s)$ with variable τ values. The green graph on the upper side of the plot is the $\Delta^{-1}(s)$ and another four graphs are the Q-filter plot with various τ values. If magnitude of $Q(s)$ is greater than $\Delta^{-1}(s)$, the inequality equation (5.8) doesn't satisfies any more. From the graph, when the $\tau = 0.1$, we can see that Q diagram intrudes the $\Delta^{-1}(s)$ in frequency range from 10 rad/s to 35 rad/s. This means when DOB faces outer disturbances with those frequency range, system could be fail. But Q plot with τ over 0.25 doesn't intrude $\Delta^{-1}(s)$. The boundary of the τ should be in the range between 0.1 and 0.25, but in conservative point of view with consideration of safety factor, we can define that system is stable with τ over 0.25 value. But too high amount of τ in Q-filter makes the filtering performance poor, so $\tau = 0.25$ will be selected afterwards.

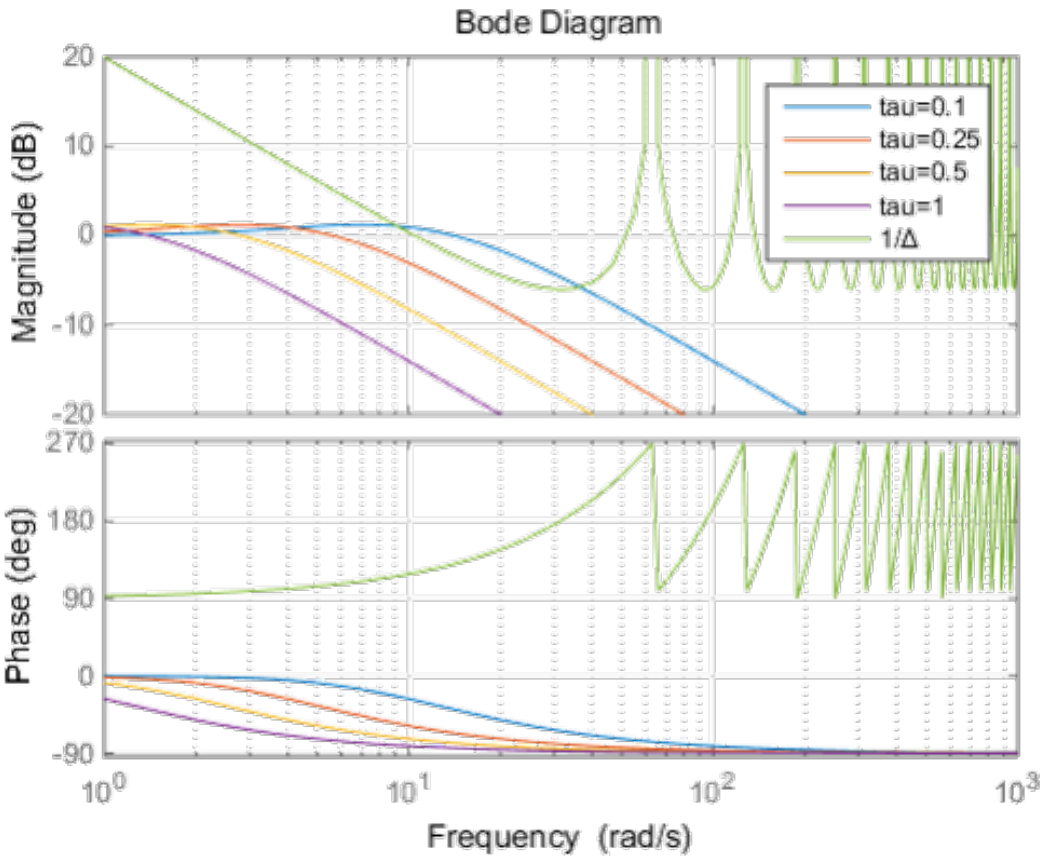

Figure 5.4: Bode diagram of the Δ^{-1} and Q with various τ values

6

Simulation Result

In this chapter, the flight simulation result of hexarotor UAV with DOB structure will be introduced. The simulation has been done by Matlab software. The robotic toolbox under courtesy of professor Peter Corke in Queensland University of Technology in Australia is used for environment setting. The cascade controller with position controller, attitude controller are implemented. See Figure 6.1.

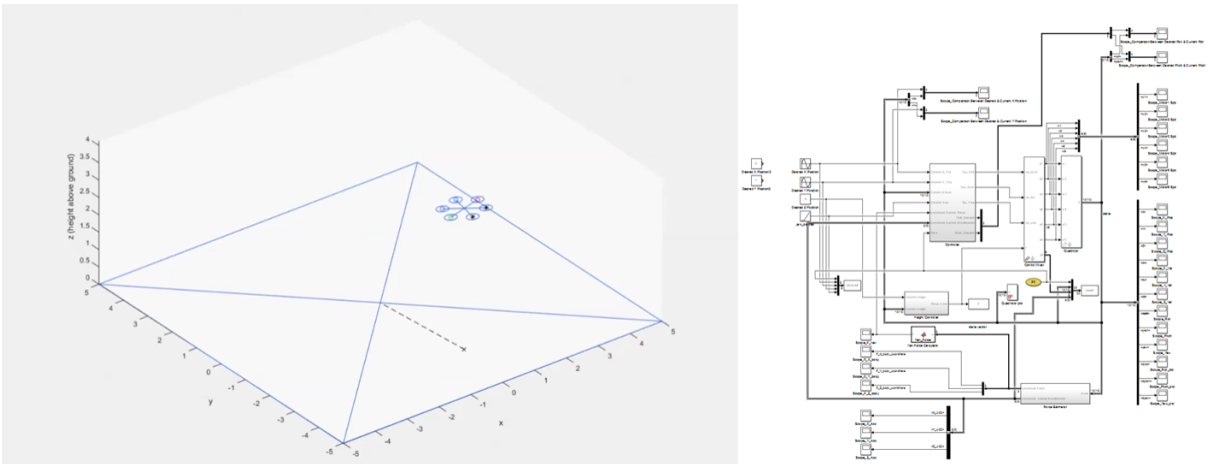

Figure 6.1: Still cut image of the hexarotor UAV's simulation flight(left), flight control structure composed in Matlab simulink(right)

With the simulation, the performance of the proposed controller is evaluated and compared with non-DOB applied situation. The inertia matrix in simulation is given by

$$J = \begin{bmatrix} 0.0282 & 0 & 0 \\ 0 & 0.0282 & 0 \\ 0 & 0 & 0.0282 \end{bmatrix}$$

.

The controller is separated into three groups, one the height controller that generates u_1, another yaw controller that controls yaw angle seperately, and finally the x and y inertial acceleration controller. See the Figure 6.2 for result. The disturbance model is combination of trigonometric function, ranging from -5 to 2.5. Figure 6.2(upper) shows the x and y inertial axial flight path log of both DOB-Off and DOB-On situation. Hexarotor drone in DOB-On situation seems to follow the desired path better than DOB-Off situation. Seeing Figure 6.3, the estimation value of the disturbance in first few seconds was oscillated but after four seconds, it well follows the real disturbance value. This means that disturbance is well estimated and cancels the outer disturbance with good performance.

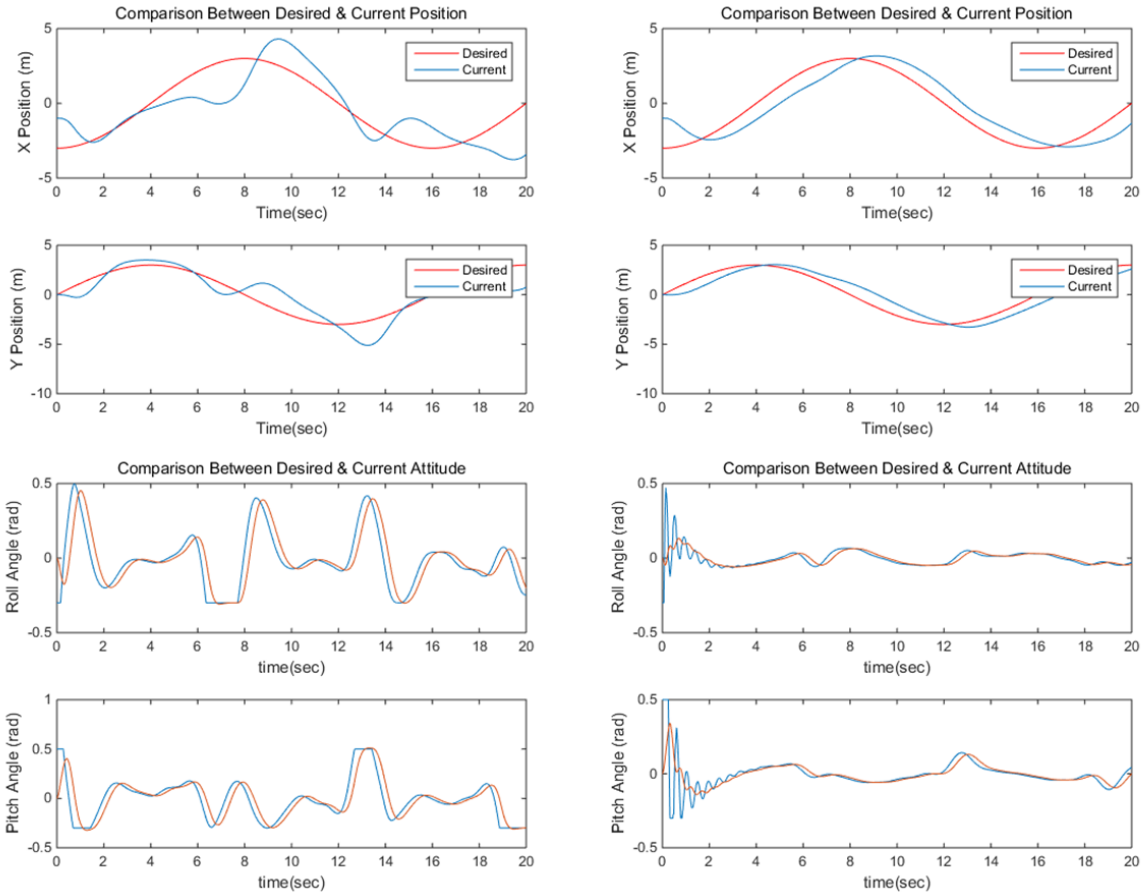

Figure 6.2: Comparison between hexarotor UAV's desired and current states: no DOB(upper left), with DOB(upper right), attitude trajectory: no DOB(lower left), with DOB(lower right)

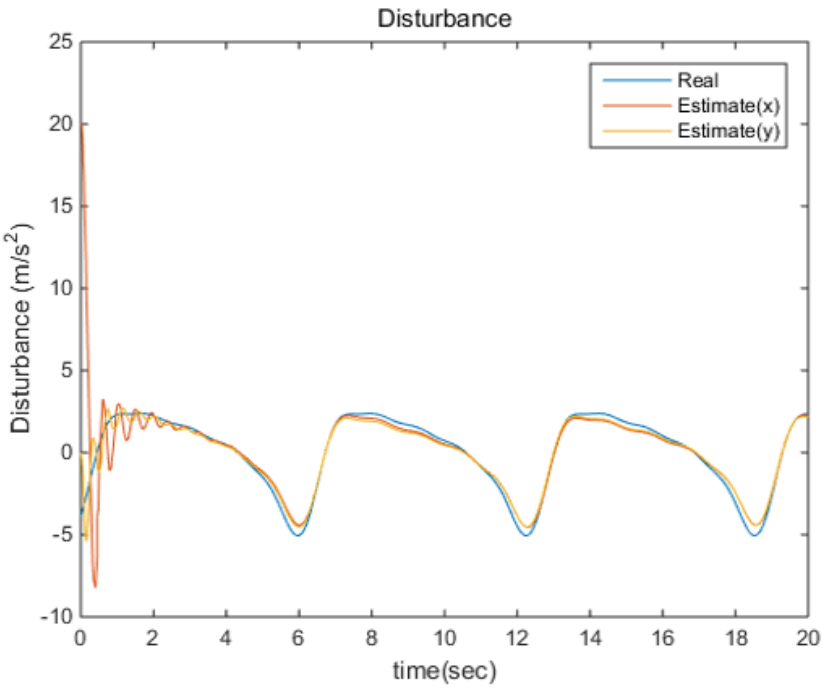

Figure 6.3: Comparison of the real disturbance and the estimated disturbances

7

Experimental Result

In this chapter, verification of the proposed control structure will be shown by actual experimental result. For experiment, modified hexarotor platform is used. With help of the electronic devices such as onboard computer or INS, and control code based on C++, the hexarotor UAV kept 100Hz of refresh rate in attitude control, 66Hz of refresh rate in position control.

7.1 Hardware Introduction and Experiment Settings

The hexarotor UAV experiment has been done by self-constructed hexarotor based on DJI's F550 platform. The flight control program is also self-constructed with Hardkernel's Odroid U3 onboard linux computer. For PWM signal generation, Arduino Uno is used. The main specifications are listed in Table 7.1.

The test environment of DOB-Off and DOB-On situation is same. The goal of the experiment is to maintain inertial coordinate's $(0, 0)$ position. The outer loop controller(position controller) is PID controller. Same setting as the simulation, the height and heading angle control are done by independent controller. DOB structure is applied into the inertial coordinate's x and y position controller only. To provide outer disturbance, the tether attached into the hexarotor UAV's arm is used and manually pulled with randomness to apply outer disturbances. Since we set manual disturbance to apply in single axial direction of the drone, the estimation result of the disturbance

Table 7.1: Main specifications of the hexarotor UAV used in experiment

Weight	3.99Kg
Maximum Thrust	10.8Kg (1.8Kg in each motor)
Blade Size	12inch.
Flight Computer	Hardkernel Odroid U3+I/O Shield
IMU	Microstrain GX3-45
Guidance	Vicon Motion Capture Device
Operation Voltage	22.2V(3.7V/Cell, 6 Cell)

acceleration should be shown in single direction. In Figure 7.1, the green block indicates the hexarotor drone. And yellow block indicates the tether attached into the hexarotor UAV for generation of the outer disturbances.

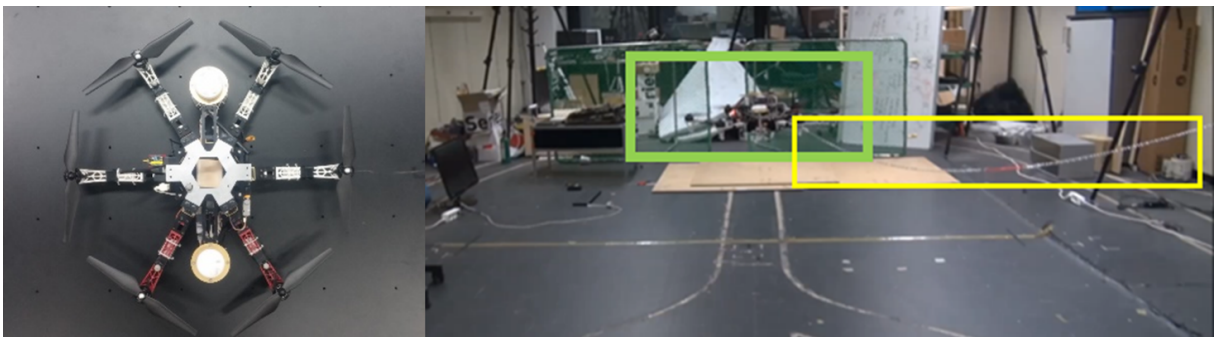

Figure 7.1: The hexarotor UAV used in experiment(left), still cut image of experiment(right)

7.2 Experimental Result

Figure 7.2 shows an experimental result of the position DOB applied in the hexarotor UAV's flight controller. The position log with DOB-Off state shows that it didn't kept its desired position but moved to positive x axial direction. In DOB-On mode however, we can observe that the hexarotor UAV's position is settled in nearby desired position even though the outer disturbance is still engaged. Figure 7.3(left) shows the magnitude of the estimated inertial coordinate in inertial x

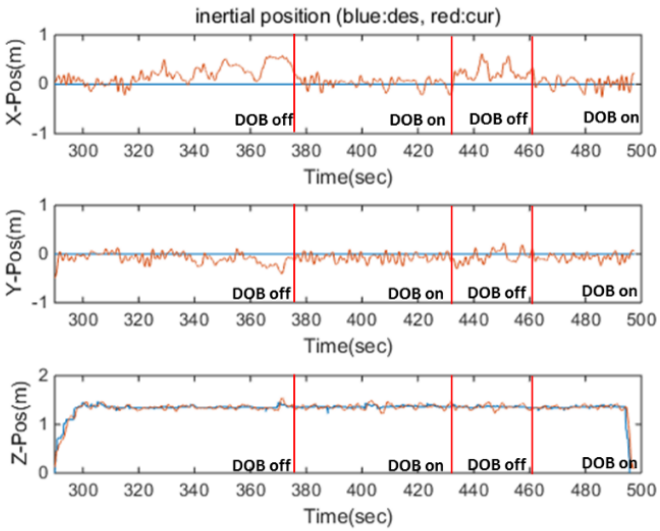

Figure 7.2: Position log of desired and current position w and w/o acceleration DOB

and y directional estimated disturbance. Figure 7.3(right) shows the comparison result between raw acceleration command coming from the position controller, and disturbance compensated acceleration command by DOB structure. As we can find out in Figure 7.3(left), the estimated disturbance plot is biased to positive x direction because teather-applied disturbance force's direction is positive inertial coordinate's x axial direction. This phenomena is also shown in Figure 7.3(right). In this figure, no blue line is shown until 370 seconds, because the DOB was turned off. Without DOB, there is no difference between u_r and u. But after 370 seconds, the DOB turned on and red signal shows the tendency to bias into negative x direction making opposite directional force to outer disturbance. Since there is minor disturbance in inertial y axis, small difference between u_r and u was observed.

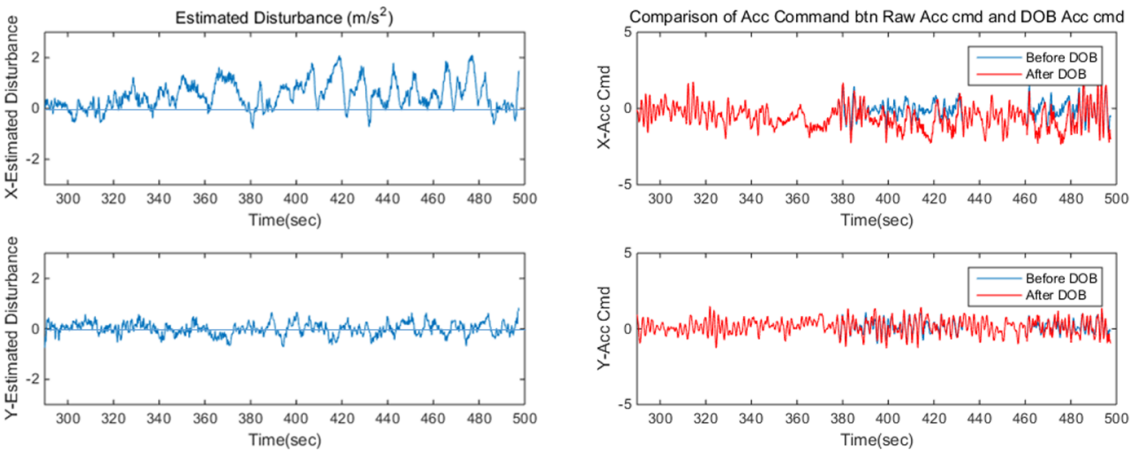

Figure 7.3: Estimated disturbance(left), raw and DOB applied acceleration command(right)

8 Conclusion

In this dissertation, robust control method using DOB structure to the acceleration control of the hexarotor UAV for outer disturbance rejection is introduced. This structure can deal with inertial coordinate's axial x and y directional disturbances such as atmospheric disturbances that we can face during the outdoor flight with harsh windy condition. Unlike some other control method, the DOB structure predicts the size of the outer disturbances and compensates, making system stable and reliable.

The kinematics and the dynamics of the system are covered in Chapter 2. In Chapter 3, the acceleration control method of the hexarotor UAV is introduced. After that, the application of the DOB structure into acceleration control is introduced in Chapter 4. The stability analysis of the proposed structure using small gain theorem is covered in Chapter 5. Both simulation and actual experiment are conducted for verification of the system in Chapter 6 and 7.

Due to the DOB methodology's basic trait, it could be redirected into another purposes such as slung load's reaction force rejection, which is generated due to the oscillation of the slung mass. Or it can also be used for multiple drone's cooperative activity such as co-lifting the object since each drone should have to deal with internal force that affects the position control of the drone.

Da.H.

References

[1] Bolandi, Hossein, et al. "Attitude control of a quadrotor with optimized pid controller." (2013).

[2] Yun, Yu, et al. "High performance full attitude control of a quadrotor on SO (3)." Robotics and Automation (ICRA), 2015 IEEE International Conference on. IEEE, 2015.

[3] Chirarattananon, Pakpong, et al. "Wind disturbance rejection for an insect-scale flapping-wing robot." Intelligent Robots and Systems (IROS), 2015 IEEE/RSJ International Conference on. IEEE, 2015.

[4] Wang, Zhenwei, et al. "Experimental verification of the model predictive control with disturbance rejection for quadrotors." Society of Instrument and Control Engineers of Japan (SICE), 2015 54th Annual Conference of the. IEEE, 2015.

[5] Voos, Ilolger. "Nonlinear control of a quadrotor micro-UAV using feedback-linearization." Mechatronics, 2009. ICM 2009. IEEE International Conference on. IEEE, 2009.

[6] Alexis, Kostas, George Nikolakopoulos, and Anthony Tzes. "Switching model predictive attitude control for a quadrotor helicopter subject to atmospheric disturbances." Control Engineering Practice 19.10 (2011): 1195-1207.

[7] Das, A. "Sliding Mode Approach to Control Quadrotor Using Dynamic Inversion, to appear as book chapter in Robust Control." (2011).

[8] Garcia, R. A., F. R. Rubio, and M. G. Ortega. "Robust PID control of the quadrotor helicopter." Advances in PID Control. Vol. 2. No. 1. 2012.

[9] Lee, Kooksun, Juhoon Back, and Ick Choy. "Nonlinear disturbance observer based robust attitude tracking controller for quadrotor UAVs." International Journal of Control, Automation and Systems 12.6 (2014): 1266-1275.

[10] Jeong, Seung H., Seul Jung, and M. Tomizuka. "Attitude control of a quad-rotor system using an acceleration-based disturbance observer: An empirical approach." Advanced Intelligent Mechatronics (AIM), 2012 IEEE/ASME International Conference on. IEEE, 2012.

[11] Dong, Wei, et al. "High-performance trajectory tracking control of a quadrotor with disturbance observer." Sensors and Actuators A: Physical 211 (2014): 67-77.

[12] Lee, Chanhwa, Youngjun Joo, and Hyungbo Shim. "Analysis of discrete-time disturbance observer and a new Q-filter design using delay function." Control, Automation and Systems (ICCAS), 2012 12th International Conference on. IEEE, 2012.

[13] Back, Juhoon, and Hyungbo Shim. "Adding robustness to nominal output-feedback controllers for uncertain nonlinear systems: A nonlinear version of disturbance observer." Automatica 44.10 (2008): 2528-2537.

[14] Shim, Hyungbo, and Young-Jun Joo. "State space analysis of disturbance observer and a robust stability condition." Decision and Control, 2007 46th IEEE Conference on. IEEE, 2007.

[15] Kempf, Carl J., and Seiichi Kobayashi. "Disturbance observer and feedforward design for a high-speed direct-drive positioning table." Control Systems Technology, IEEE Transactions on 7.5 (1999): 513-526.

[16] Artale, V., C. Milazzo, and A. Ricciardello. "Mathematical modeling of hexacopter." Appl. Math. Sci 7.97 (2013): 4805-4811.

[17] Alaimo, A., et al. "Mathematical modeling and control of a hexacopter." Unmanned Aircraft Systems (ICUAS), 2013 International Conference on. IEEE, 2013.

국 문 초 록

본 논문은 야외 환경에서 비행하는 헥사로터 무인항공기의 제어에 관한 방법을 주제로 제시하였다. 헥사로터 무인항공기의 야외 비행 시 처하게 되는 비행 환경은 실내 비행 시와는 사뭇 다른데, 이는 바람에 의한 외란 발생과 그로 인해 동체에 가해지는 의도치 않은 가속도의 발생 때문이다. 이에 따라 동체에 가해지는 의도치 않은 횡방향 외란 가속도를 상쇄하기 위하여 기존의 멀티로터 무인항공기 위치제어와는 다른 두 가지 기법이 추가되었다. 첫 번째는 헥사로터 무인항공기의 '평면 가속도 제어' 이고, 두 번째는 평면 가속도 제어기에 부착된 '외란 관측기'를 이용한 외란 상쇄이다. 먼저, 드론의 자세와 평면 가속도와의 상관관계에 관한 변환행렬식이 유도되었다. 변환행렬식을 통하여 헥사로터 무인항공기는 목표 가속도를 발생시키기 위해 인가해야 하는 목표 자세를 계산할 수 있게 되었다. 헥사로터 무인항공기가 계산된 목표 자세를 자세 제어기를 통해 추종함으로써 동체의 평면 가속도 제어가 가능케 되었다. 그 다음 평면 가속도 제어기에 외란관측기를 추가하였다. 드론의 목표 가속도 입력과 결과 가속도 사이의 전달함수를 구하고, 결과 가속도를 바탕으로 역함수를 곱하여 현재 가속도를 유발시킨 목표 가속도 입력을 계산하였다.

계산값을 실제 제어 입력과 비교하여 예상 외란 입력값을 계산하고, 다음 제어입력에서 예상치를 미리 감산하여 외란을 상쇄함으로써 드론의 결과 가속도가 목표 가속도와 최대한 유사하도록 '외란 관측기'를 구성하였다. 안정성 분석을 위해 'Small gain theorem'이 사용되었다. 'Small gain theorem' 을 통해 시스템 전체의 안정성이 유지될 수 있도록 외란 관측기에 포함되어 있는 저역 통과 필터의 대역폭을 지정할 수 있었다. 시뮬레이션과 실제 실험을 수행하였고, 이를 통해 제안된 제어 방식에 대한 유효성을 확인할 수 있었다.

주요어 : 헥사로터. 멀티로터 무인기, 강인 제어, 외란 관측기, 가속도 제어, 스몰 게인 이론

학번 : 2014-20678